# Probing the Caveolin-1 P132L Mutant: Critical Insights into Its Oligomeric Behavior and Structure

Monica D. Rieth,[†] Jinwoo Lee,[†] and Kerney Jebrell Glover*

Department of Chemistry, Lehigh University, 6 E. Packer Ave, Bethlehem, Pennsylvania 18015, United States

S *Supporting Information*

ABSTRACT: Caveolin-1 is the most important protein found in caveolae, which are cell surface invaginations of the plasma membrane that act as signaling platforms. A single point mutation in the transmembrane domain of caveolin-1 (proline 132 to leucine) has deleterious effects on caveolae formation *in vivo* and has been implicated in various disease states, particularly aggressive breast cancers. Using a combination of gel filtration chromatography and analytical ultracentrifugation, we found that a fully functional construct of caveolin-1 ($Cav1_{62-178}$) was a monomer in dodecylphosphocholine micelles. In contrast, the P132L mutant of $Cav1_{62-178}$ was dimeric. To explore the dimerization of the P132L mutant further, various truncated constructs ($Cav1_{82-178}$, $Cav1_{96-178}$, $Cav1_{62-136}$, $Cav1_{82-136}$, $Cav1_{96-136}$) were prepared which revealed that oligomerization occurs in the transmembrane domain (residues 96−136) of caveolin-1. To characterize the mutant structurally, solution-state NMR experiments in *lyso*-myristoylphosphatidylglycerol were undertaken of the $Cav1_{96-136}$ P132L mutant. Chemical shift analysis revealed that, compared to the wild-type, helix 2 in the transmembrane domain was lengthened by four residues (wild-type, residues 111−129; mutant, residues 111−133), which corresponds to an extra turn in helix 2 of the mutant. Lastly, point mutations at position 132 of $Cav1_{62-178}$ (P132A, P132I, P132V, P132G, P132W, P132F) revealed that no other hydrophobic amino acid can preserve the monomeric state of $Cav1_{62-178}$, which indicates that proline 132 is critical in supporting proper caveolin-1 behavior.
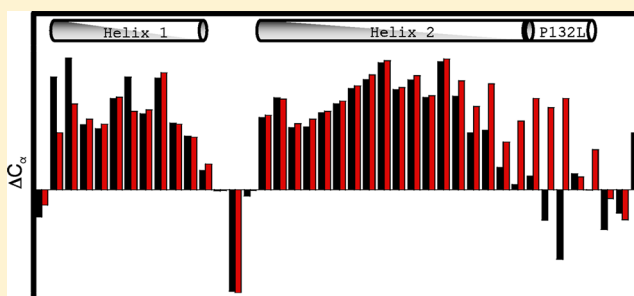
Caveolae are indentations of the plasma membrane of mammalian cells that are approximately 50−100 nm in diameter.[1] These microdomains are intimately involved in numerous cellular functions ranging from signal transduction to lipid recycling.[2] Caveolae are ubiquitous and can be found in most terminally differentiated cell types, notably smooth muscle cells and adipocytes.[1] Caveolae are primarily comprised of a protein called caveolin, which is critical for the formation of caveolae. It is estimated that approximately 100−200 caveolin proteins are present in a single caveola, and studies have shown that when the caveolin gene is silenced, caveolae disappear from the surface of cells.[3,4] Caveolin is an integral membrane protein, and ∼50% of the polypeptide chain is predicted to interact with the plasma membrane. Glycosylation mapping, limited proteolysis, and cell surface biotinylation studies have demonstrated that the N- and C-termini of caveolin reside on the cytosolic side of the membrane.[5−7] The transmembrane region of caveolin is ∼33 amino acids in length, which is significantly longer than the 20−25 amino acids required to span the plasma membrane. In addition, there are no soluble amino acids present in the transmembrane region of caveolin that would facilitate a polytopic orientation. Taken together, these findings have led to the postulation that caveolin forms a horseshoe-like loop in the membrane (Figure 1). The horseshoe-like loop conformation is believed to facilitate the high degree of membrane curvature observed in caveolae.[4] Furthermore, the membrane curvature is believed to be
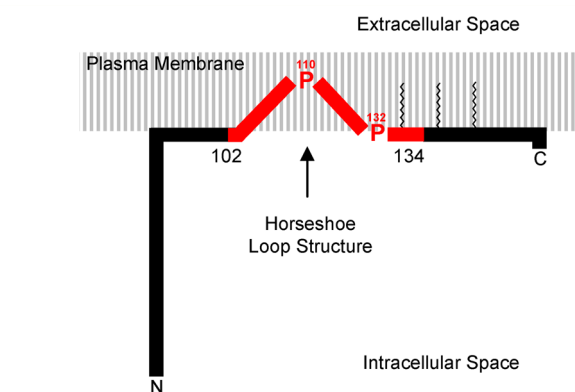
Figure 1. Cartoon of caveolin-1 topology. The transmembrane domain is highlighted in red. The zigzag lines represent sites of cysteine palmitoylation.

stabilized by the formation of high molecular weight caveolin oligomers.

Caveolin has been closely linked to a number of disease states including heart disease, Alzheimer's, and cancer. Specifically, a naturally occurring point mutation (P132L) in

the caveolin-1 gene is present in ∼16% of breast cancers and has been closely linked to increased recurrence and metastasis.[8,9] In addition, this mutant appears to be functionally different from the wild-type as it is retained in the Golgi apparatus of cells and does not get transported to its final destination in the plasma membrane. The expression of the P132L mutant results in the elimination of caveolae from the surface of cells.[10] Interestingly, the P132L mutant appears to behave in a dominant negative manner: When both the P132L mutant and wild-type caveolin are coexpressed, both become localized to the Golgi, which is a fate common to misfolded proteins.[10] Furthermore, a study by Bonuccelli et al. demonstrates that when caveolin-1 P132L is expressed in Met-1 cells, it acts as a loss-of-function mutation and promotes recurrence of breast cancer.[8]

In this report, we examine both the oligomeric and secondary structural changes that occur in the caveolin-1 P132L mutant versus wild-type caveolin-1. Using gel filtration chromatography and sedimentation equilibrium analytical ultracentrifugation, we show that the P132L mutant is dimeric compared to the wild-type which is monomeric. Using various truncated constructs, we have isolated the dimerization region to the transmembrane domain which is where the P132L mutation resides. In addition, we show that substitution of proline 132 with 6 other nonpolar amino acids does not disrupt dimerization, which reveals the importance of proline at position 132. Using chemical shift indexing NMR analysis, we found that the putative re-entrant helix of the P132L mutant is extended by 4 additional amino acids which results in a longer α-helix when compared to the wild-type. Furthermore, the NMR studies reveal that the P132L point mutation results in only a localized change to the transmembrane region of caveolin rather than a global conformation change.

■ MATERIALS AND METHODS

Protein Expression and Purification. The DNA for Cav1$_{62-178}$ was synthesized by Genscript Corporation (Piscataway, NJ). Caveolin-1 has three sites of cysteine palmitoylation (C133, C143, C156) that have been shown to be nonessential for proper caveolin-1 folding and trafficking.[11−13] Therefore, each cysteine was mutated to serine to avoid unwanted and biologically irrelevant disulfide bonding. The Cav1$_{62-178}$ gene was cloned, overexpressed, and purified as described in Diefenderfer et al.[14] After HPLC purification, 30 mg of dried Cav1$_{62-178}$ was dissolved in 3 mL of hexafluoroisopropanol followed by the addition of 7 mL of deionized water. The solution was flash frozen and lyophilized. MALDI-TOF analysis confirmed the identity of the final protein product. The truncated wild-type and P132L mutant constructs prepared were Cav1$_{82-178}$, Cav1$_{82-136}$, Cav1$_{96-178}$, Cav1$_{96-136}$, Cav1$_{62-136}$. The point mutation constructs prepared were Cav1$_{62-178}$: P132A, P132G, P132W, P132F, P132V, P132I. The truncated and point mutation constructs were expressed and purified using the same procedure described above.

Expression of Isotopically Labeled Protein. The expression of uniformly labeled ^{15}N and ^{13}C Cav1$_{96-136}$ P132L was prepared as described in Marley et al.[15] Labeled amino acids were incorporated by expressing Cav1$_{96-136}$ P132L according to the procedure outlined in Truhlar et al.[16]

Gel Filtration Chromatography. To 0.8 mg of lyophilized Cav1$_{62-178}$, 1.0 mL of buffer (20 mM HEPES pH 7.4, 150 mM NaCl, and 50 mM DPC (Anatrace, Maumee, OH)) was added followed by 3 min of vigorous vortexing. Next, the resultant

clear solution was filtered through a 0.2 μm spin filter and injected onto a Sephacryl-300HR 16/60 column (GE Healthcare, Piscataway, NJ) equilibrated with buffer (20 mM HEPES pH = 7.4, 150 mM NaCl and 5 mM DPC). The column was calibrated using alcohol dehydrogenase, carbonic anhydrase, β-amylase, bovine serum albumin, and cytochrome c oxidase, and the elution profile was monitored at 280 nm. All truncated and point mutation constructs were run in an identical fashion to the wild-type and mutant Cav1$_{62-178}$.

Analytical Ultracentrifugation. 0.8 mg of lyophilized Cav1$_{62-178}$ was reconstituted into a density-matched buffer comprised of 20 mM HEPES pH 7.4, 100 mM NaCl, 50 mM DPC, and 52.5% (v/v) D$_2$O. DPC micelles were matched using a D$_2$O concentration of 52.5% (v/v) in a solution of 20 mM HEPES, 100 mM NaCl pH = 7.4.[17] Each protein sample was prepared at three concentrations (30, 15, and 7.5 μM) and verified using the BCA Assay (Pierce Protein Research Products, Rockford, IL). The samples were loaded into a six-sector charcoal-filled Epon centerpiece (path length 1.2 cm) using the DPC buffer solution above without protein as the reference solution. The volume of sample per sector was 120 μL. The cells were loaded in a Beckman Ti-60 four-hole rotor. Equilibrium absorbance measurements were taken at three speeds, and the data were analyzed by global nonlinear least-squares fitting using the computer program "HeteroAnalysis Version 1.1.0.44 - beta" (University of Connecticut).[18] Cav1$_{62-178}$ was fit to the ideal model to obtain the weight-averaged molecular weight of the protein. During fitting, all parameters (molecular weight, baseline, and reference concentration) were allowed to float. Mutant Cav1$_{62-178}$ P132L was fit to a "monomer-Nmer" model (where N was fixed to a value of 2). Again, all parameters (molecular weight, baseline, and reference concentration) were allowed to float. The partial specific volumes of the wild-type and mutant Cav1$_{62-178}$ were calculated using established methodology (0.7603 and 0.7615 mL/g, respectively).[19] The density of the DPC buffer (1.0592 g/mL) was determined using a Kyoto Electronics density/specific gravity meter (model #DA-210).

NMR Sample Preparation. To 2.5 mg of lyophilized Cav1$_{96-136}$ P132L, 500 μL of LMPG buffer was added (100 mM LMPG, 100 mM NaCl, 20 mM phosphate pH 7, 10% D$_2$O) for a final protein concentration of 1 mM. The sample was vortexed vigorously and briefly heated (∼1 min) in a water bath until clear. The clear solution was spin filtered in a 0.2 μm filter to remove any particulates. The NMR spectrum was acquired at 37 °C using a 600 MHz Bruker Advance II NMR spectrometer (Billerica, MA) equipped with a cryoprobe. For backbone assignments TROSY-based HSQC, HNCA, and HN(CO)CA experiments were performed. Specific amino acid labeling (valine, serine, leucine) was used to clarify ambiguous peaks. The spectra were processed using NMRPipe and Sparky.[20,21] Secondary structure information was obtained using Cα chemical shifts as described in Wishart et al.[22] Dihedral angles for wild-type Cav1$_{96-136}$ were obtained using the computer program TALOS+.[23] For TALOS+ H, N, CO, Cα, and Cβ chemical shift data were used.

■ RESULTS AND DISCUSSION

For studies of caveolin-1 oligomerization we chose a construct that encompasses residues 62−178 (Cav1$_{62-178}$). *In vivo* studies have shown that when the first 65 amino acids were deleted from caveolin-1, it had a behavior that was indistinguishable from that of the full-length protein.[24] This strongly indicates
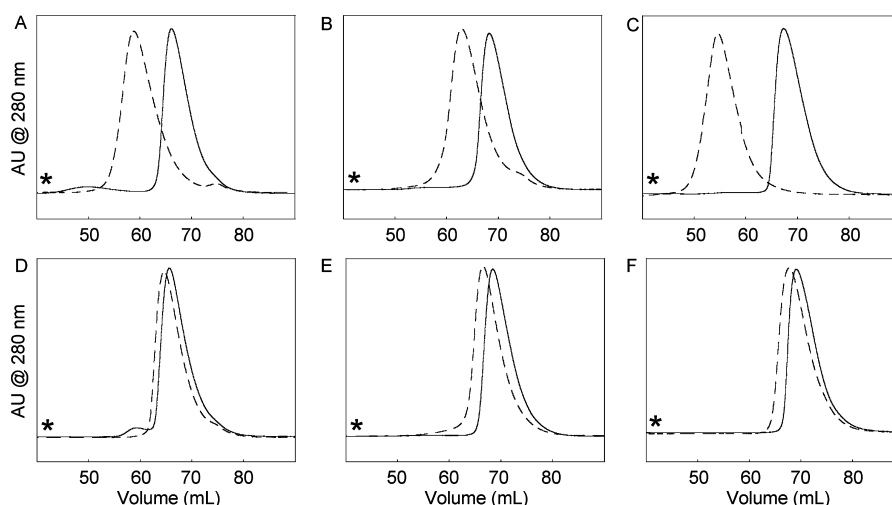
Figure 2. Gel filtration chromatograms of various caveolin-1 constructs: (A) $Cav1_{62-178}$, (B) $Cav1_{82-178}$, (C) $Cav1_{96-178}$, (D) $Cav1_{62-136}$, (E) $Cav1_{82-136}$, and (F) $Cav1_{96-136}$. Solid line represents wild-type. Dashed line represents the P132L mutant. Asterisk denotes the void volume.
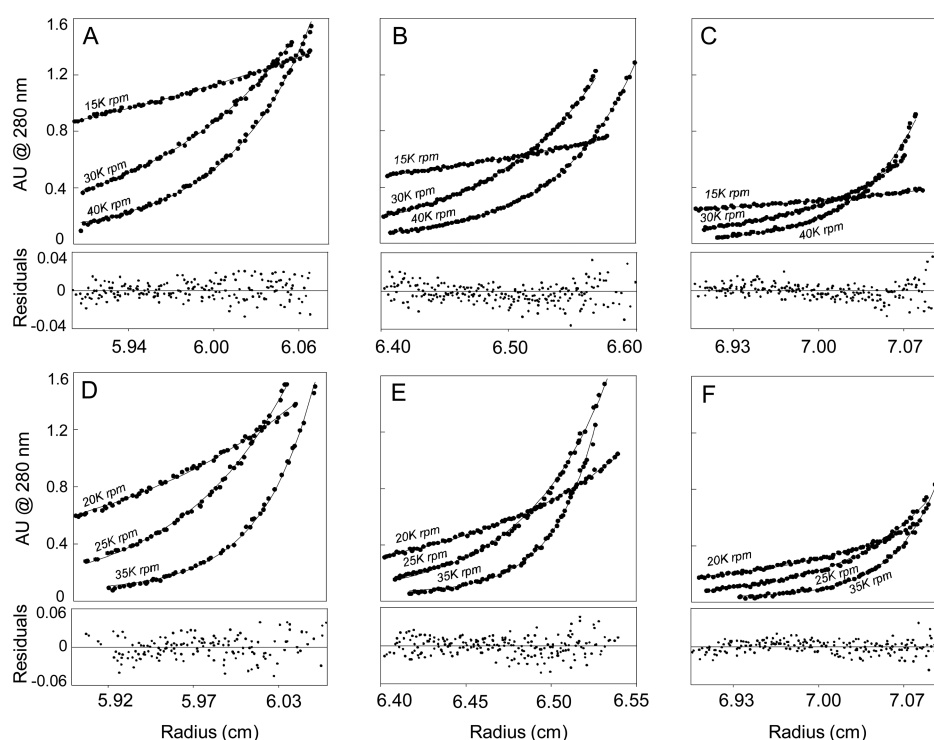

Figure 3. Sedimentation equilibrium profiles of $Cav1_{62-178}$ and $Cav1_{62-178}$ P132L. Panels A−C represent the $Cav1_{62-178}$ at concentrations of 30, 15, and 7.5 μM, respectively. Panels D−F represent $Cav1_{62-178}$ P132L at concentrations of 30, 15, and 7.5 μM, respectively. Both wild-type and mutant were evaluated at three speeds which have been overlaid in each panel.

that $Cav1_{62-178}$ retains the crucial structural elements necessary for full caveolin-1 function.

Wild-type $Cav1_{62-178}$ was reconstituted into a buffer containing dodecylphosphocholine (DPC) micelles. DPC micelles are a very native-like membrane mimic that are used widely in a variety of biophysical membrane protein experiments.[25−27] When reconstituted $Cav1_{62-178}$ was subjected to gel filtration analysis, a single symmetrical peak was observed (Figure 2A, solid line). The presence of a single symmetrical peak indicates that a homogeneous oligomeric population of the protein is present and that $Cav1_{62-178}$ is *not* forming multiple oligomeric states. In addition, $Cav1_{62-178}$ did not elute in the void volume, revealing that the column retained

separation ability. Therefore, if multiple $Cav1_{62-178}$ oligomeric states were present, gel filtration would have resolved them. When the gel filtration column was calibrated with known globular protein standards, the $Cav1_{62-178}$ fraction had an apparent molecular weight of 115 kDa. On the basis of these results, caveolin-1 forms only one predominant oligomeric state.

Next, mutant $Cav1_{62-178}$ P132L was subjected to gel filtration analysis. The mutant also eluted as a single, symmetrical, nonvoided peak indicating that a homogeneous oligomeric population was present (Figure 2A, dashed line). However, the mutant eluted before the wild-type, indicating that it was present in a larger oligomeric state. In contrast to the wild-type,
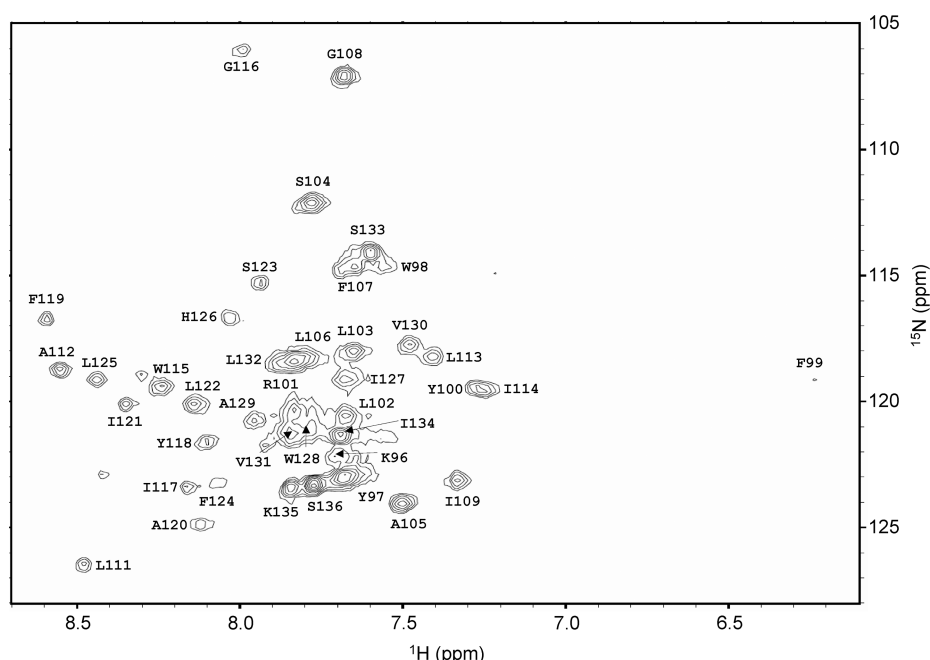
Figure 4. $^1H-^{15}N$ TROSY HSQC spectrum of Cav1$_{96-136}$ P132L. The spectrum was acquired with 256 complex points in t1 (^{15}N) and 2048 complex points in t2 (^1H).

the mutant had an apparent molecular weight of 190 kDa. However, gel filtration analysis does not give us definitive information about the precise oligomeric state of the wild-type and mutant Cav1$_{62-178}$: This is due to the fact that DPC molecules are bound to Cav1$_{62-178}$, which can dramatically inflate the apparent molecular weight. Also, membrane protein−detergent complexes may not be globular, which can inflate the molecular weight as well.

To overcome the limitations of gel filtration analysis, wild-type and mutant Cav1$_{62-178}$ were subjected to analysis by analytical ultracentrifugation. The method of sedimentation equilibrium was employed because it is a very powerful approach for determining the molecular weight of membrane proteins in detergent solutions. Importantly, sedimentation equilibrium experiments give molecular weight information that is independent of molecular shape. In addition, sedimentation equilibrium experiments can be run under density-matched conditions, which allows for the detergent contribution to the observed molecular weight to be eliminated.[28−30] Therefore, using this method, the exact oligomeric state of wild-type and mutant Cav1$_{62-178}$ can be characterized.

Figure 3 summarizes the data from the analytical ultracentrifugation experiments of both the wild-type and the P132L mutant. For wild-type Cav1$_{62-178}$ (Figure 3A−C), the data were fit to the ideal, single species model. It was clear from the gel filtration experiments that only one oligomeric population was present for both the wild-type and mutant Cav1$_{62-178}$. After fitting the sedimentation profile of Cav1$_{62-178}$ to the ideal model, the reported molecular weight was 14 606 ± 19 Da. This value is reported with 617 degrees of freedom and a root-mean-square deviation of 0.011. This agrees very well with the calculated molecular weight of the wild-type monomer which is 13 450 Da. (The ~1 kDa discrepancy can be attributed to the inherent inaccuracy of predicting partial specific volumes of proteins in detergent solutions.) On the basis of these results, it is clear that caveolin-1 is a monomer and does not homooligomerize at all. Therefore, it is unlikely that the observed

SDS-resistant high molecular weight complexes previously reported for caveolin-1 are simply a result of caveolin-1 homooligomerizing.[6] Clearly, the mechanism of caveolae formation is more complex and likely involves other biomolecules such as cholesterol. In fact, caveolin-1 has been shown to closely associate with cholesterol *in vivo*; therefore, the appearance of these high molecular weight complexes may be due to the presence of SDS resistant caveolin−cholesterol aggregates.[6] It is important to note that SDS is a much more powerful detergent toward protein deaggregation than DPC, which is much milder. Considering this, it is highly unlikely that DPC would interfere with caveolin-1 oligomerization. Additionally, studies suggesting caveolin-1 oligomerizes are based heavily on the behavior of fragments of caveolin from the N-terminal and scaffolding domains.[6,24,31] It is not clear from these studies whether the fragments were representative of the native caveolin-1 protein. In one report the studies were performed in the absence of a membrane mimic which is not representative of caveolin-1's membrane environment. Our studies reveal that when a *fully functional* construct of caveolin-1 (Cav1$_{62-178}$) is analyzed in a membrane environment, it does not form high-order oligomers and is in fact monomeric. This result helps to clarify the role of caveolin-1 in caveolae.

Next, mutant Cav1$_{62-178}$ P132L was subjected to analysis by analytical ultracentrifugation (Figure 3D−F). Initially, the data were fitted to the ideal species model the same way that the wild-type data were fitted. The observed molecular weight was 28 282 Da. This value is approximately twice the molecular weight of the P132L monomer, 13 465 Da, showing that a dimeric species was present. Next, we explored the possibility of a monomer−dimer equilibrium by fitting the data to a monomer−dimer model. Upon fitting, the observed molecular weight of the monomer was 14 079 ± 55 Da. This value is reported with 1420 degrees of freedom and a root-mean-square deviation of 0.015. This number corresponds very well to the calculated molecular weight of the P132L monomer (13 465 Da). In addition, the model produced a dissociation constant of
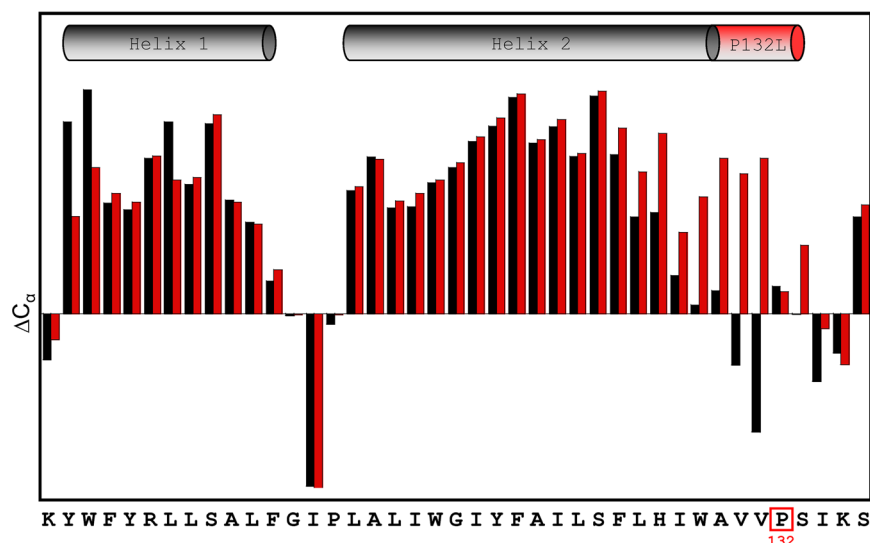
Figure 5. Chemical shift analysis of Cav1$_{96-136}$ and Cav1$_{96-136}$ P132L. Wild-type is depicted with black bars, and the mutant is depicted with red bars. Cav1$_{96-136}$ P132L shows an extension of helix 2 by four residues.

15 nM, which shows that the dimer is quite stable. We take this dissociation constant to be the upper limit. We believe the dissociation constant is actually much less than 15 nM because at the concentrations used in these studies no monomeric caveolin-1 was observed. From these results, we conclude that the P132L mutant forms stable dimers in a membrane-like environment unlike the wild-type which is monomeric.

After determining that the oligomeric state of the P132L mutant was dimeric, the region of Cav1$_{62-178}$ P132L that was responsible for the observed dimerization was investigated. Caveolin-1 is typically described as having four distinct domains: an N-terminal domain (residues 62−81), a scaffolding domain (residues 82−95), a transmembrane domain (residues 96−136), and a C-terminal domain (residues 137−178). Therefore, the following truncated constructs of both the wild-type and mutant caveolin-1 were generated: Cav1$_{62-136}$, Cav1$_{82-136}$, Cav1$_{82-178}$, Cav1$_{96-136}$, and Cav1$_{96-178}$. Importantly, all constructs contained the intact transmembrane domain (residues 96−136). Each of the five constructs was analyzed by gel filtration chromatography, and the elution profiles of both wild-type and P132L were compared (Figure 2B−F). In all five cases, the P132L mutant elutes before the wild-type, indicating that a larger oligomeric species was present. Since all of the truncated constructs contained the intact transmembrane domain, and all truncated constructs elute before the wild-type, these results indicate that the dimerization region lies in the transmembrane domain of caveolin-1 where the P132L mutation is found.

Next, NMR structural studies were undertaken to observe the changes that occur in the transmembrane domain of the wild-type versus the P132L mutant. Figure 4 shows the HSQC spectrum of mutant Cav1$_{96-136}$ P132L. Line widths are broader when compared to the wild-type spectrum reported in Lee et al.[32] This observed line broadening is consistent with oligomerization. When the N, H, CO, Cα, and Cβ chemical shifts for the wild-type Cav1$_{96-136}$ were inputted into the computer program TALOS+, residues Y97−V131 were confidently predicted to have a dihedral angle, and residues P132−K135 were predicted to be dynamic.[23] Table 1 in the Supporting Information provides a complete list of the TALOS+ data. Importantly, the prediction of the wild-type

secondary structure in TALOS+ matched the secondary structure prediction using only Cα chemical shift data. Therefore, we used the Cα chemical shift indexing to reveal the secondary structure of Cav1$_{96-136}$ P132L. Chemical shift indexing (Figure 5) of Cα reveals that the transmembrane domain still retains the four distinct regions previously observed for the wild-type caveolin transmembrane domain: There is an α-helix from residues 97−107 (helix 1), a break from residues 108−110, another α-helix from residues 111−129 (helix 2), and an unstructured region from residues 130−136.[32] Consistent with the horseshoe topology model of caveolin, the break at residues 108−110 is likely where the turn occurs so that the polypeptide chain can return to the membrane surface. Clearly in the case of the mutant, the break is not lost so it is unlikely that this mutant disrupts the proposed horseshoe topology. In addition, helix 1 is unaffected as well. However, helix 2 is extended by 4 residues to encompass residues 111−133. Therefore, there is approximately one extra helical turn in the mutant. The unstructured region now begins at residue 134 for the mutant rather than residue 130 for the wild-type. This increased helicity is likely forming a dimerization domain in the transmembrane domain in close proximity to position 132 (Figure 6). In the native protein, residue P132 causes helix 2 to terminate at residue 129 which prevents the dimerization from occurring. Therefore, the helix-breaking tendency of proline is employed to prevent the dimerization of caveolin-1. Figure 6 shows a model of how caveolin-1 dimerization may occur. This model is an extension of the original model of caveolin-1 presented by Hancock and Parton, which was based entirely on primary sequence analysis and not on biophysical data.[4] Our model shows that when the proline is removed from position 132 the unstructured region begins at residue 134 instead of residue 130. We believe this lengthening of helix 2 opens up an interface that leads to the dimerization of caveolin-1, which was observed in the analytical ultracentrifugation study. The purpose of our model is to highlight this dimerization interface. Although other dimerization models consistent with the association around position 132 can be built, we present only one model for brevity. Clearly, more studies to definitively characterize the structure of the dimer will be needed.
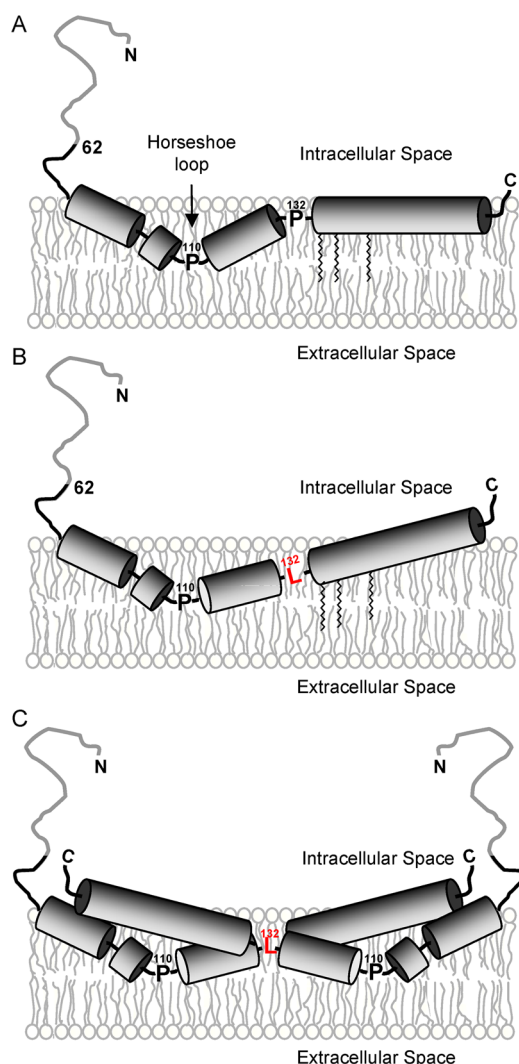
Figure 6. (A) Model of caveolin-1 in the plasma membrane. (B) Model of caveolin-1 P132L mutant in the plasma membrane. (C) Model of the caveolin-1 P132L dimer.

Next, specific hydrophobic amino acid substitutions were made at position 132 to determine whether other hydrophobic amino acids could substitute for proline at the 132 position. We chose to substitute the following residues: isoleucine (P132I), valine (P132V), alanine (P132A), glycine (P132G), tryptophan (P132W), phenylalanine (P132F). Each residue is nonpolar so it does not affect the properties of $Cav1_{62-178}$ by significantly changing the hydrophobicity. Each of these mutants was examined by gel filtration chromatography and compared to the wild-type and mutant $Cav1_{62-178}$. On the basis of the elution profiles of the mutants, we can see that all of them elute before the wild-type (Figure 7), showing that all of the mutants retain dimerization capabilities. The P132A, P132G, P132I, and P132V mutants had slightly longer retention times compared to the P132L mutant when run at a constant flow rate, indicating that the dimerization may be somewhat weaker for some of the point mutants. Clearly, it appears that proline is the only amino acid that is tolerated at position 132, and it further explains why proline is conserved in all three caveolin isoforms.

As stated in the Introduction, the mutation of P132L in caveolin-1 results in a variety of disease states. However, there has been little characterization of the differences between the wild-type and the mutant at the atomic level. Importantly, our data show that wild-type caveolin-1 is monomeric and does not form high-order oligomers. Therefore, the high-order oligomers that have been reported for caveolin-1 are likely due to other proteins/factors that are present *in vivo*. In contrast, the P132L mutant spontaneously dimerizes. This dimerization could explain why the mutant is retained in the Golgi apparatus *in vivo* and does not reach its final destination in the plasma membrane. Furthermore, it is likely that other factors are at play and are contributing to the creation of the caveolin oligomers observed *in vivo*. Also, given that processes in the cell are tightly regulated, it is reasonable to think that for proper cellular transport caveolin-1 must be in a monomeric state and then once it reaches the plasma membrane other factors such as cholesterol, or the protein PTRF/cavin could trigger the oligomerization. Recent studies have shown that caveolin closely associates with the protein, PTRF/cavin. In fact, when
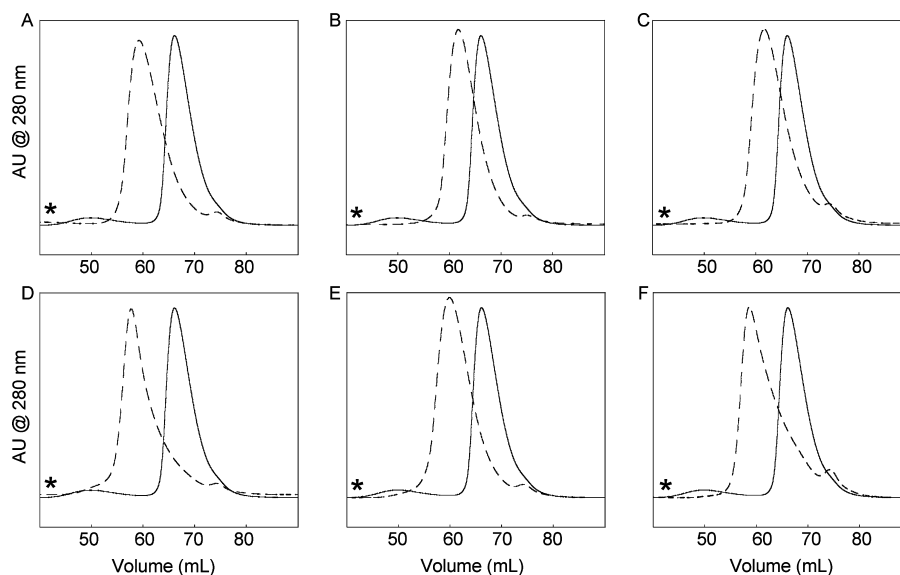
Figure 7. Gel filtration chromatograms of the caveolin-1 P132X mutants: (A) P132I, (B) P132G, (C) P132A, (D) P132F, (E) P132V, and (F) P132W. The dashed line represents the P132X mutant, and the solid line represents the wild-type. Asterisk denotes the void volume.

the PTRF/cavin gene is silenced, the number of caveolae in the plasma membrane diminishes.[33] The P132L mutant, on the other hand, dimerizes which may not be the proper oligomeric state for trafficking to the plasma membrane, and could explain why it is retained in the Golgi apparatus. Proline is a very unique amino acid because it is conformationally rigid. Because of this rigidity, proline is known to be helix breaking. This could be critical for caveolin-1 as P132 is located toward the end of the transmembrane domain where the protein is transitioning from a near-vertical helix in the membrane to the C-terminal domain, which is an amphipathic helix that is predicted to reside horizontally on the membrane surface. When the proline is removed, the second helix of the transmembrane domain is extended by one turn. This small change is significant enough to open up a dimerization domain in helix 2 (Figure 6). No other nonpolar amino acids can be substituted for proline, indicating how critical this residue is in supporting proper caveolin-1 behavior.

■ ASSOCIATED CONTENT

ⓢ Supporting Information

TALOS+ data (Table 1) for wild-type Cav1$_{96-136}$. This material is available free of charge via the Internet at http://pubs.acs.org.

■ AUTHOR INFORMATION

Corresponding Author

*Phone 1-610-758-5081; Fax 1-610-758-6536; e-mail kjg206@lehigh.edu.

Author Contributions

[†]The authors contributed equally to the work presented in this paper.

Notes

The authors declare no competing financial interest.

■ ACKNOWLEDGMENTS

■ ABBREVIATIONS

NMR, nuclear magnetic resonance spectroscopy; DPC, dodecylphosphocholine; LMPG, lysomyristoylphosphatidylglycerol; SDS, sodium dodecyl sulfate.

■ REFERENCES

(1) Lisanti, M. P., and Williams, T. M. (2004) The Caveolin Genes: From Biology to Medicine. *Annu. Med. 36*, 584−595.

(2) Spisni, E., Tomasi, V., Cestaro, A., and Tosatto, S. C. (2005) Structural Insights into the Function of Human Caveolin 1. *Biochem. Biophys. Res. Commun. 338*, 1383−1390.

(3) Drab, M., Verkade, P., Elger, M., Kasper, M., Lohn, M., Lauterbach, B., Menne, J., Lindschau, C., Mende, F., Luft, F. C., Schedl, A., Haller, H., and Kurzchalia, T. V. (2001) Loss of Caveolae, Vascular Dysfunction, and Pulmonary Defects in Caveolin-1 Gene-Disrupted Mice. *Science 293*, 2449−2452.

(4) Parton, R. G., Hanzal-Bayer, M., and Hancock, J. F. (2006) Biogenesis of Caveolae: A Structural Model for Caveolin-Induced Domain Formation. *J. Cell. Sci. 119*, 787−796.

(5) Monier, S., Dietzen, D. J., Hastings, W. R., Lublin, D. M., and Kurzchalia, T. V. (1996) Oligomerization of VIP21-Caveolin in Vitro is Stabilized by Long Chain Fatty Acylation Or Cholesterol. *FEBS Lett. 388*, 143−149.

(6) Sargiacomo, M., Scherer, P. E., Tang, Z., Kubler, E., Song, K. S., Sanders, M. C., and Lisanti, M. P. (1995) Oligomeric Structure of Caveolin: Implications for Caveolae Membrane Organization. *Proc. Natl. Acad. Sci. U. S. A. 92*, 9407−9411.

(7) Dupree, P., Parton, R. G., Raposo, G., Kurzchalia, T. V., and Simons, K. (1993) Caveolae and Sorting in the Trans-Golgi Network of Epithelial Cells. *EMBO J. 12*, 1597−1605.

(8) Bonuccelli, G., Casimiro, M. C., Sotgia, F., Wang, C., Liu, M., Katiyar, S., Zhou, J., Dew, E., Capozza, F., Daumer, K. M., Minetti, C., Milliman, J. N., Alpy, F., Rio, M. C., Tomasetto, C., Mercier, I., Flomenberg, N., Frank, P. G., Pestell, R. G., and Lisanti, M. P. (2009) Caveolin-1 (P132L), a Common Breast Cancer Mutation, Confers Mammary Cell Invasiveness and Defines a Novel Stem cell/metastasis-Associated Gene Signature. *Am. J. Pathol. 174*, 1650−1662.

(9) Williams, T. M., and Lisanti, M. P. (2005) Caveolin-1 in Oncogenic Transformation, Cancer, and Metastasis. *Am. J. Physiol.: Cell Physiol. 288*, C494−C506.

(10) Lee, H., Park, D. S., Razani, B., Russell, R. G., Pestell, R. G., and Lisanti, M. P. (2002) Caveolin-1 Mutations (P132L and Null) and the Pathogenesis of Breast Cancer - Caveolin-1 (P132L) Behaves in a Dominant-Negative Manner and Caveolin-1 (−/−) Null Mice show Mammary Epithelial Cell Hyperplasia. *Am. J. Pathol. 161*, 1357−1369.

(11) Uittenbogaard, A., and Smart, E. J. (2000) Palmitoylation of Caveolin-1 is Required for Cholesterol Binding, Chaperone Complex Formation, and Rapid Transport of Cholesterol to Caveolae. *J. Biol. Chem. 275*, 25595−25599.

(12) Dietzen, D. J., Hastings, W. R., and Lublin, D. M. (1995) Caveolin is Palmitoylated on Multiple Cysteine Residues. Palmitoylation is Not Necessary for Localization of Caveolin to Caveolae. *J. Biol. Chem. 270*, 6838−6842.

(13) Sotgia, F., Razani, B., Bonuccelli, G., Schubert, W., Battista, M., Lee, H., Capozza, F., Schubert, A. L., Minetti, C., Buckley, J. T., and Lisanti, M. P. (2002) Intracellular Retention of Glycosylphosphatidyl Inositol-Linked Proteins in Caveolin-Deficient Cells. *Mol. Cell. Biol. 22*, 3905−3926.

(14) Diefenderfer, C., Lee, J., Mlyanarski, S., Guo, Y., and Glover, K. J. (2009) Reliable Expression and Purification of Highly Insoluble Transmembrane Domains. *Anal. Biochem. 384*, 274−278.

(15) Marley, J., Lu, M., and Bracken, C. (2001) A Method for Efficient Isotopic Labeling of Recombinant Proteins RID A-7811−2009. *J. Biomol. NMR 20*, 71−75.

(16) Truhlar, S. M., Cervantes, C. F., Torpey, J. W., Kjaergaard, M., and Komives, E. A. (2008) Rapid Mass Spectrometric Analysis of 15N-Leu Incorporation Fidelity during Preparation of Specifically Labeled NMR Samples. *Protein Sci. 17*, 1636−1639.

(17) Losonczi, J. A., Olejniczak, E. T., Betz, S. F., Harlan, J. E., Mack, J., and Fesik, S. W. (2000) NMR Studies of the Anti-Apoptotic Protein Bcl-xL in Micelles. *Biochemistry 39*, 11024−11033.

(18) Cole, J. L. (2004) Analysis of Heterogeneous Interactions. *Methods Enzymol. 384*, 212−232.

(19) Cohn, E. J., and Edsall, J. J. (1943) *Proteins, Amino Acids, and Peptides as Ions and Dipolar Ions*, p 375, Reinhold Pub. Corp., New York.

(20) Goddard, T. D., and Kneller, D. G. *SPARKY3*, University of California, San Francisco.

(21) Delaglio, F., Grzesiek, S., Vuister, G. W., Zhu, G., Pfeifer, J., and Bax, A. (1995) NMRPipe: A Multidimensional Spectral Processing System Based on UNIX Pipes. *J. Biomol. NMR. 6*, 277−293.

(22) Wishart, D., and Sykes, B. (1994) The C-13 Chemical-Shift Index - a Simple Method for the Identification of Protein Secondary Structure using C-13 Chemical-Shift Data. *J. Biomol. NMR 4*, 171−180.

(23) Shen, Y., Delaglio, F., Cornilescu, G., and Bax, A. (2009) TALOS+: A Hybrid Method for Predicting Protein Backbone Torsion Angles from NMR Chemical Shifts. *J. Biomol. NMR 44*, 213−223.

(24) Machleidt, T., Li, W. P., Liu, P., and Anderson, R. G. (2000) Multiple Domains in Caveolin-1 Control its Intracellular Traffic. *J. Cell Biol. 148*, 17−28.

(25) Neumoin, A., Arshava, B., Becker, J., Zerbe, O., and Naider, F. (2007) NMR Studies in Dodecylphosphocholine of a Fragment Containing the Seventh Transmembrane Helix of a G-Protein-Coupled Receptor from Saccharomyces Cerevisiae. *Biophys. J. 93*, 467−482.

(26) Zamoon, J., Mascioni, A., Thomas, D. D., and Veglia, G. (2003) NMR Solution Structure and Topological Orientation of Monomeric Phospholamban in Dodecylphosphocholine Micelles. *Biophys. J. 85*, 2589−2598.

(27) Beswick, V., Guerois, R., Cordier-Ochsenbein, F., Coic, Y. M., Tam, H. D., Tostain, J., Noel, J. P., Sanson, A., and Neumann, J. M. (1999) Dodecylphosphocholine Micelles as a Membrane-Like Environment: New Results from NMR Relaxation and Paramagnetic Relaxation Enhancement Analysis. *Eur. Biophys. J. 28*, 48−58.

(28) Fleming, K. G. (2008) Determination of Membrane Protein Molecular Weight using Sedimentation Equilibrium Analytical Ultra-centrifugation. *Curr. Protoc. Protein Sci.*, Unit 7.12.1−7.12.13.

(29) Reynolds, J., and Tanford, C. (1976) Determination of Molecular Weight of the Protein Moiety in Protein-Detergent Complexes without Direct Knowledge of Detergent Binding. *Proc. Natl. Acad. Sci. U. S. A. 73*, 4467−4470.

(30) Mayer, G., Ludwig, B., Muller, H., van den Brook, J. A., Friesen, R. H. E., and Schubert, D. (1999) Studying Membrane Proteins in Detergent Solution by Analytical Ultracentrifugation: Different Methods for Density Matching. *Prog. Colloid Polym. Sci. 113*, 176−181.

(31) Fernandez, M. A., Albor, C., Ingelmo-Torres, M., Nixon, S. J., Ferguson, C., Kurzchalia, T., Tebar, F., Enrich, C., Parton, R. G., and Pol, A. (2006) Caveolin-1 is Essential for Liver Regeneration. *Science 313*, 1628−1632.

(32) Lee, J., and Glover, K. J. (2012) The Transmembrane Domain of Caveolin-1 Exhibits a Helix-Break-Helix Structure. *Biochim. Biophys. Acta 1818*, 1158−1164.

(33) Liu, L., Brown, D., McKee, M., Lebrasseur, N. K., Yang, D., Albrecht, K. H., Ravid, K., and Pilch, P. F. (2008) Deletion of Cavin/PTRF Causes Global Loss of Caveolae, Dyslipidemia, and Glucose Intolerance. *Cell Metab. 8*, 310−317.